Hindawi
Geofluids
Volume 2023, Article ID 2197400, 8 pages
https://doi.org/10.1155/2023/2197400

Research Article

Experimental Study on Water-Rock Interaction Characteristics of Unconsolidated Sandstone during CO_2 Multicomponent Thermal Fluid Injection

Mingzhe Guo,[1,2] **Zengmin Lun**,[1] **Bing Zhou**,[1] **Lianguo Wang**,[2] **and Huiqing Liu**[1,2]

[1]*Petroleum Exploration & Production Research Institute, Sinopec, Beijing, China*
[2]*State Key Laboratory of Petroleum Resources and Prospecting, China University of Petroleum (Beijing), Beijing 102249, China*

Correspondence should be addressed to Zengmin Lun; lunzm.syky@sinopec.com

Received 28 September 2022; Revised 7 December 2022; Accepted 31 March 2023; Published 25 April 2023

Academic Editor: Ze Wang

According to the reservoir characteristics and the current situation of CO_2 utilization during thermal recovery in an unconsolidated sandstone heavy oil reservoir, the mechanism and law of porosity and permeability change in an unconsolidated sandstone heavy oil reservoir during CO_2+steam and CO_2+steam+ sodium alpha-olefin sulfonate (AOS) injection were studied by combining a static monomineral water-rock reaction and a dynamic polymineral sand pack displacement experiment. In the static water-rock reaction between CO_2 and monomineral of reservoir rock, the dissolution degree of monomineral at 200°C is greater than that at 100°C and 300°C, and the order of mineral dissolution is illite, montmorillonite, kaolinite, and quartz. Besides, the dissolution rate of single rock minerals decreased significantly in the system of CO_2 with AOS. In the polymineral sand pack displacement experiment, the porosity gradually decreases by CO_2 multicomponent thermal fluid, and the permeability first decreases and then increases by CO_2 multicomponent thermal fluid, but the permeability change is only about 0.5% by CO_2+steam+ AOS, which is mainly attributed to the adsorption of AOS on the rock surface, and it is confirmed in the infrared spectrum of unconsolidated sand after displacement. This also shows that CO_2+steam+AOS can stabilize the rock skeleton structure of the reservoir and prevent the deterioration of heterogeneity in the subsequent development of thermal recovery of heavy oil reservoirs; therefore, the CO_2 multicomponent thermal fluid with chemical agents can improve the damage of a single CO_2 thermal fluid to the reservoir.

1. Introduction

Presently, the increasingly severe climate crisis is another serious test in front of all mankind, requiring all sectors of the world to work together to deal with it, of which fossil energy combustion contributes nearly 67% of the global greenhouse gases [1]. For heavy oil, which is the main supply of fossil energy, the CO_2 multicomponent thermal fluid injection method will be one of the main technologies to reduce carbon dioxide emissions [2, 3]. The carbon dioxide injection is not only to reduce carbon emissions but also to increase crude oil production, which will be the ultimate goal of the CO_2 multicomponent thermal fluid injection method in heavy oil reservoirs [4, 5]. During thermal recovery, the dissolution and transformation of minerals such as quartz and clay near the wellbore occur under a pressure of 12 MPa and a temperature of 300°C [6].

In comparison, the influence of temperature and pH on mineral corrosion is stronger than that of ionic strength and pressure under dynamic conditions, so the coinjection of CO_2 and steam will cause the dissolution of reservoir quartz and the transformation of clay minerals [7, 8]. The chemical changes in reservoir rock structure and composition cause the cementation strength of the weakly consolidated rock to weaken again, so that the reservoir framework fines can migrate under a little shearing action [9, 10]. With the increase of CO_2 and steam injection volume, the skeleton fines continue to peel off, migrate, and flow out, which expands the pore throat radius of the reservoir and further causes steam channelling. As shown in Figure 1, the

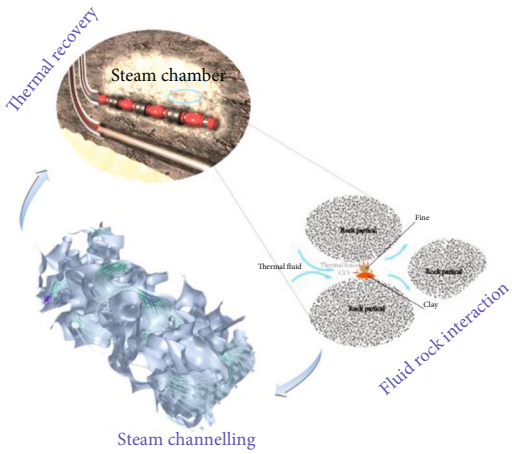

Figure 1: Schematic diagram of reservoir damage during thermal fluid flooding.

Table 1: Initial experimental parameters.

Name	Value	Unit
Salinity of formation water	12000	Mg/L
Pressure after steam injection	4.2	MPa
Crude oil viscosity	996	mPa·s
Average content of clay	12%	
Average reservoir porosity	32.7%	
Average permeability	729.1	mD

formation of the reticulate steam thief region will affect production and make CO_2 storage and utilization less than expected. Previous studies have shown that CO_2 foam can reduce interlayer and intralayer interference and improve the steam displacement effect of a heterogeneous reservoir [11–13]. And foam can slow down the rapid breakthrough of CO_2 to achieve the purpose of thermal CO_2 flooding. Although studies on the physical properties of reservoir rocks caused by the interaction of steam+CO_2 with reservoir rocks have been reported, the study did not mention the effects of thermal force, chemical agent, and gas on the skeleton of the reservoir rock. It is particularly important to study the variation law of reservoir porosity and permeability during multicomponent thermal fluid injection [14, 15].

The CO_2 multicomponent thermal fluid injection method is an enhanced oil recovery technology after single steam injection in weakly consolidated sand reservoirs. With the application of the CO_2 multicomponent thermal fluid injection method, steam channelling intensifies, and sand production near the well area is serious [16, 17]. In addition, the time effect of the water shutoff and controlling profile is short during controlling steam channelling [18]. Thus, we need to understand the porosity and permeability of unconsolidated sandstone using the CO_2 multicomponent thermal fluid injection method. Then, we should study further the interaction between the CO_2 multicomponent thermal fluid and reservoir rock minerals to analyse the mechanism causing the result. According to the physical properties and rock composition of the Zheng 364 reservoir in Shengli Oilfield, the change rules of the reservoir physical properties in CO_2 multicomponent thermal fluid were studied through the water-rock experiment of monomineral, and the mechanism of reservoir physical property change in CO_2 multicomponent thermal fluid was analysed to supplement the mechanism of enhanced oil recovery of the CO_2 multicomponent thermal fluid injection method.

2. Materials and Methods

The experimental instruments were a high-temperature and high-pressure reactor, QBZY-2 interfacial tension meter, Zeiss Sigma 500 field emission scanning electron microscope, Bruke V70 Fourier transform infrared spectrometer, MS603TS/02 electronic balance and ISCO pump, and other displacement equipment.

The surfactant used in the experiment is an anionic surfactant, sodium α-alkenyl sulfonate (AOS) of analytical grade provided by Sinopharm Chemical Reagent Co., Ltd. The monolithic minerals quartz, montmorillonite, illite, and kaolinite are all provided by Hebei Mineral Powder Processing Factory to provide rock blocks and ore powder, including 80 meshes of quartz and 200 meshes of montmorillonite, illite, and kaolinite.

The formation water in the study area is of the $CaCl_2$ type, and the Ca^{2+} concentration is 288 mg/L; the Mg^{2+} concentration is 75 mg/L. The initial parameters of the experiment are shown in Table 1.

2.1. Determination of Optimal Concentration of Surfactant. The oil-water interfacial tension was measured by using the QBZY-2 interfacial tension meter stabilized at a room temperature of 25°C for 20 min, and the foaming volume of AOS at different concentrations was observed for a comprehensive determination of the optimal concentration.

2.2. Monolithic Mineral Hydrothermal Reactions. The surface of the monolithic mineral rock block is polished with a grinding wheel and then rinsed with distilled water; then, the rock block is dried in a drying box at 80°C, and then the four mineral rock blocks are soaked in formation water for 24 hours. Take out the rock blocks and put them into the reaction kettle and fill the whole chamber with distilled water, then adjust the pressure of the reaction kettle to 4.2 MPa, set the temperature to 100°C, 200°C, and 300°C, respectively, and reciprocate the cycle of heating and cooling and introducing CO_2. After 72 hours of reaction, the rock blocks were taken out, rinsed with distilled water, dried at 80°C, weighed, and the percentage of mass change was calculated, which was recorded as the amount of dissolution. Similarly, the distilled water was replaced with the AOS solution at the optimum concentration for the above operations.

2.3. Dynamic Reaction Evaluation. The rock skeleton volume is calculated according to the porosity of the reservoir. Then the quartz density is used to estimate the mass of quartz sand required to achieve this porosity, and finally, a sand pack model with a diameter of 16 mm and a length of 50 mm is made by mixing and filling according to the clay

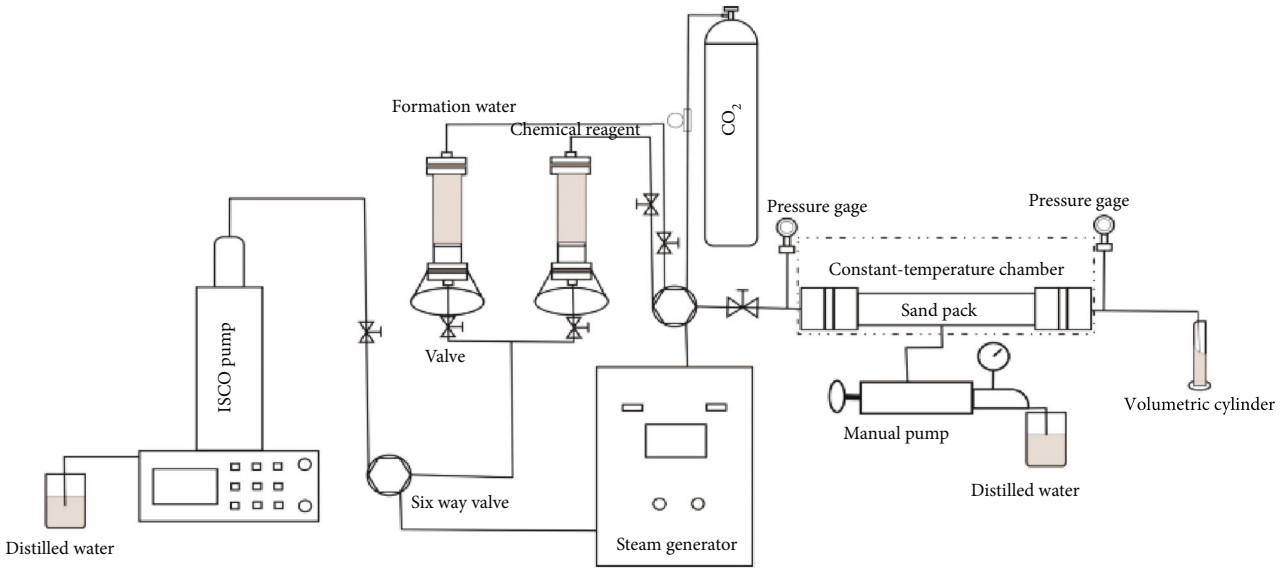

Figure 2: CO_2 multicomponent thermal fluid flooding process.

content contained. Install the instrument as shown in Figure 2, dry the sand pack model, weigh it, vacuum it to saturate the simulated formation water for 8 hours, and weigh it again to calculate the porosity and pore volume. Different temperature steam+CO_2 and steam+CO_2+surfactant AOS flooding experiments were conducted at 0.1 mL/min and inject 200 PV volume multiples. Then, open the nitrogen gas to remove the air in the pipeline, ventilate for 5 minutes to discharge the air and steam condensed water in the sand-filling model, select the inlet and outlet pressure values that meet the conditions of Darcy's law, and then record the atmosphere through the soap film flowmeter. Finally, the gas permeability was calculated by Darcy's formula; the porosity was still measured by saturation weighing. After the flooding, collect the sand sample for scanning with an electron microscope.

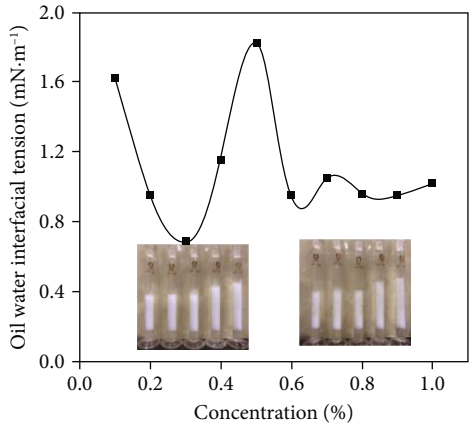

Figure 3: Oil-water interfacial tension of AOS solution at different concentrations.

3. Results and Discussion

3.1. Primary Selection of Surfactant Concentration. Anionic surfactant AOS has good salt resistance, acid and alkali resistance, and temperature resistance characteristics and is a good material for auxiliary chemical agents for thermal recovery. In order to express the experimental effect, parameters such as the foaming effect of aqueous solutions with different concentrations of AOS and the oil-water interfacial tension were evaluated. Ten mass concentrations of 0.1%, 0.2%, 0.3%, 0.4%, 0.5%, 0.6%, 0.7%, 0.8%, 0.9%, and 1% were selected for evaluation, and the results are shown in Figure 3.

With the increase of the concentration, the foaming effect of AOS is getting better and better, and the foam volume increases gradually, but the changing trend of the oil-water interfacial tension is to decrease first and then increase, from 0.1% to 0.3%; the oil-water interfacial tension decreases rapidly. According to the mechanism of surfactant reducing oil-water interfacial tension, the number of AOS molecules adsorbed at the oil-water interface also increases with the increase of concentration and spreads out at the interface one by one, so the interfacial tension decreases [19]. The critical micelle concentration is reached when the molecules spread across the interface, and as the concentration of AOS increases, the number of molecules also begins to increase. At the same temperature, the AOS molecules continue to compete with the AOS molecules at the interface for adsorption, resulting in a change in the interface spreading morphology. This affects the interfacial energy, so the oil-water interfacial tension increases when the concentration exceeds 0.3% [20]. So, the optimal concentration of AOS is 0.3%.

3.2. Static Single Rock Water-Rock Reaction. As shown in Figure 4(a), at 100°C, the mass loss of illite in the CO_2 and distilled water medium is the largest, followed by montmorillonite and kaolinite, and quartz is the least. Although CO_2 is an acid gas, the surface reaction of this mineral is extremely slow. However, the dissolution degree of each

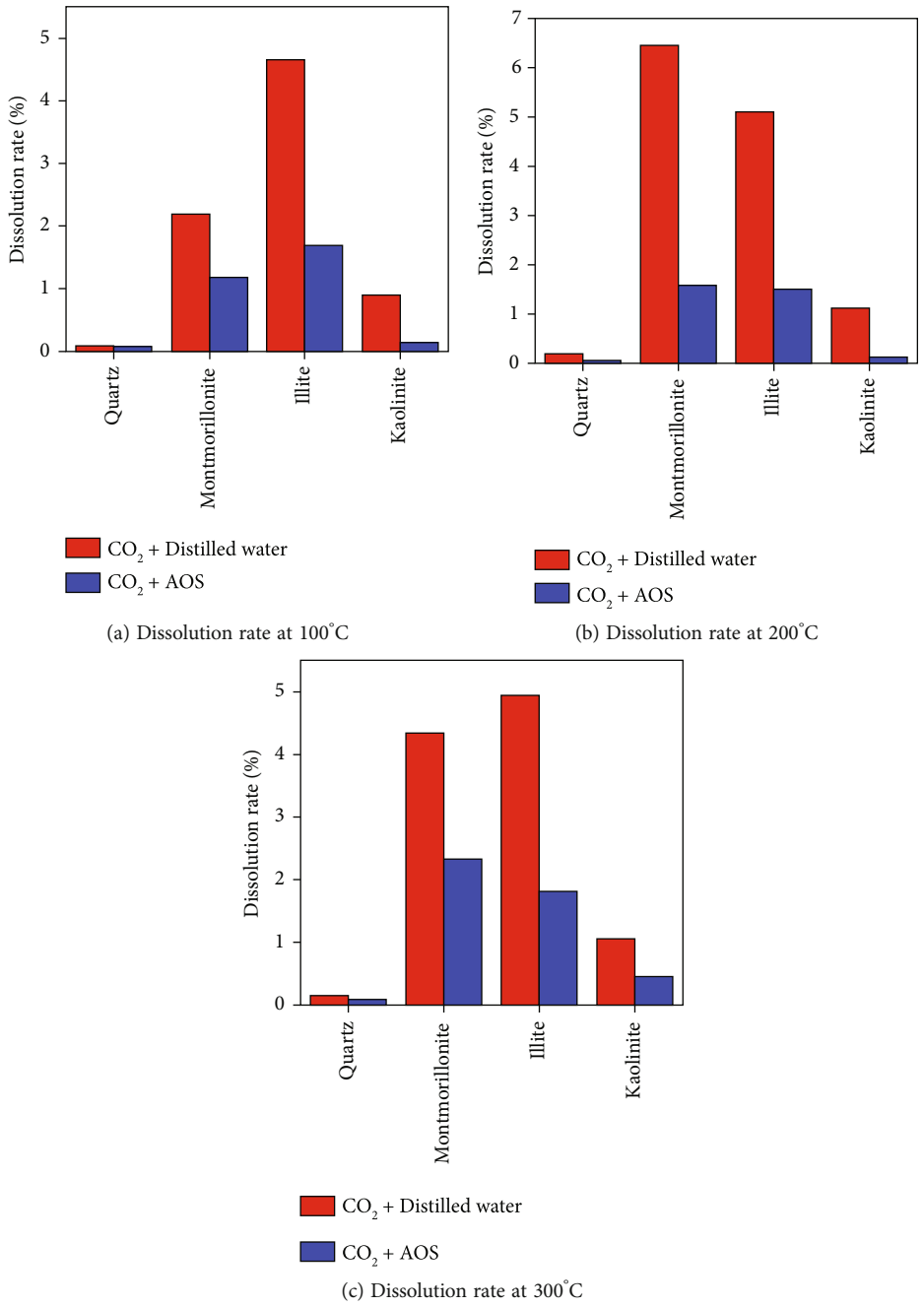

Figure 4: The dissolution rate of minerals at different temperature conditions.

mineral decreases after adding AOS, which indicates that the effect of thermal and CO_2 decreases. As shown in Figure 4(b), when the temperature reaches 200°C, the corrosion amount of illite and montmorillonite is significantly higher than that at 100°C, and the dissolution degree of montmorillonite is higher than that of illite. This is probably because the transformation degree of montmorillonite to the illite mixed layer is higher than that of illite at 200°C. In contrast, the response of kaolinite to temperature is not strong, and AOS has an inhibitory effect on mineral dissolution [21–24]. As shown in Figure 4(c), the corrosion amount of montmorillonite and illite is also the highest, but the corrosion amount of quartz and kaolinite increases slightly. The temperature of mineral dissolution is temperature-responsive, but the response is very slow. In general, the corrosion temperature response of minerals to CO_2 is very obvious, especially clay minerals, and quartz is weaker than that. The inflection points of CO_2 corrosion and AOS inhibition of mineral dissolution at high temperatures appeared at 200°C, which may be related to the temperature response of mineral surface adsorption energy [25, 26].

3.3. Dynamic Hydrothermal Effect. Figure 5 shows the infrared spectra of scattered sand after displacement in different ways.

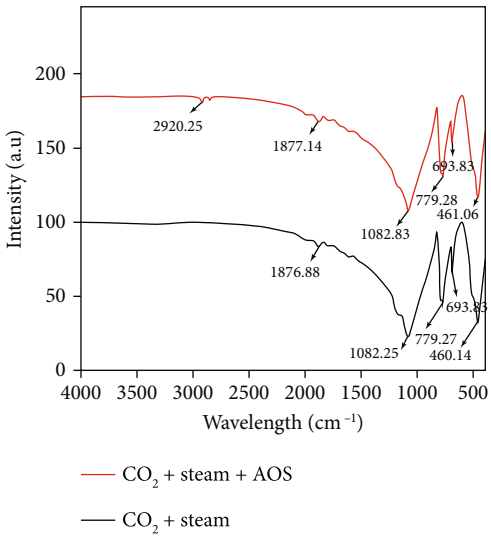

Figure 5: Infrared spectrum of sand with clay.

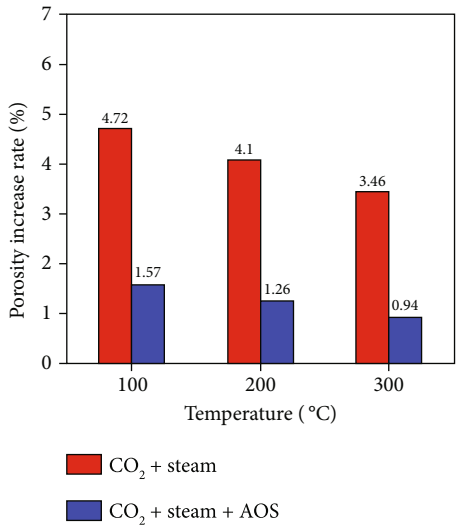

Figure 6: Results for the changes of porosity.

There is a weak C=O absorption vibration peak at 1870 cm^{-1}, and the absorption peak near 1082 cm^{-1} is the stretching vibration of the silicon-oxygen bond and the aluminium-oxygen bond. The absorption peak around 600-800 cm^{-1} is the symmetrical stretching vibration of Al-O and Si-O bonds, and the 460 cm^{-1} is the vibration and bending of the Si-O bond in-plane. However, the bending vibration peak of Si-O-Al, which should have appeared near 500 cm^{-1}, did not appear, so it was concluded that bond breaking occurred under the dual action of high temperature and CO_2. The antisymmetric stretching vibration of the methylene group appeared near 2900 cm^{-1} in the infrared spectrum after CO_2+steam+AOS. This indicates that there is organic matter adsorption in the scattered sand, i.e., AOS is adsorbed on the scattered sand.

The method for measuring porosity is the weighing method, and the benefit of this method is that it can directly reflect fines production or not and the amount of fines production. As shown in Figure 6, the rate of increase in porosity decreases with increasing temperature. The increase in porosity indicates that the volume of the framework decreases. The loss of fines decreases with the increase in temperature, which may be due to the fact that the pores of the rock are compressed at high temperatures, and the pore size decreases, so that some migrating fines cannot flow out [27, 28]. When AOS was added, the response of the porosity change was not obvious with temperature. Besides, the difference in temperature response to porosity change during CO_2+steam injection is 0.63% on average, while the difference in temperature response to porosity change during CO_2+steam+AOS injection is 0.315% on average. It can be seen that the temperature response to porosity change is reduced by half after AOS injection.

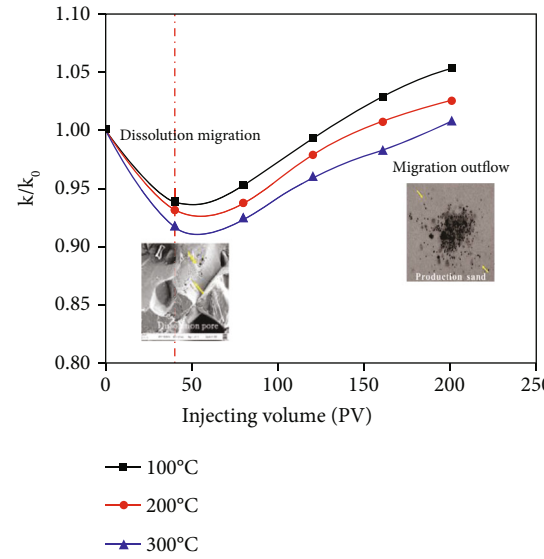

Figure 7: Changes in permeability of CO_2+steam.

3.3.1. Permeability Change. As shown in Figure 7, the permeability of the sand pack model at different temperatures first decreased and then increased, and the raise speed decreases gradually. With the increase in temperature, the degree of migration blockage increases, and the permeability recovery becomes slow. The permeability decreases within the injected volume of 40 PV, which may be due to the displacement of fines caused by fluid shear or the reduction of pore radius due to the expansion of clay due to water absorption; this effect is greater than that of fines production, thereby reducing permeability. It can be seen from the quartz electron microscope pictures of CO_2 treatment at 200°C that local pitting does occur, and the degree is not high, but it is enough to reduce the interaction force between particles. Under the action of fluid drag force, fines are easy to migrate. In general, the permeability results are reduced within the injected volume of 40 PV, and the permeability will recover and continue to increase when the fluid is continuously injected. It may be because the fines production effect is greater than the internal fines migration and expansion of clay. In addition, this permeability "recovery" is not

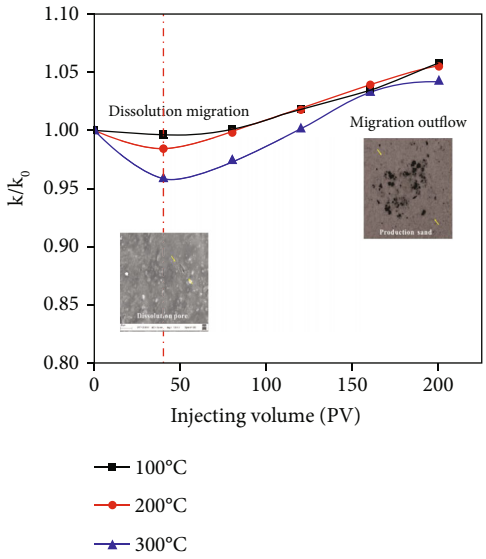

Figure 8: Changes in permeability of CO_2+steam+AOS.

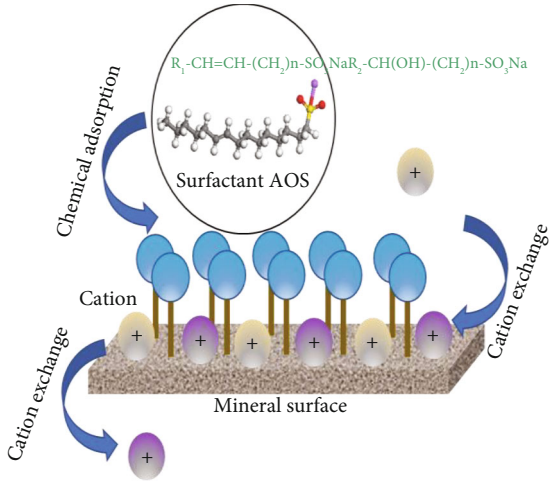

Figure 9: Rock protects the mechanism of CO_2+steam+AOS.

only negative but also means channelling of injection fluid, which can even aggravate the sand production degree near the well. The permeability "recovery" becomes slower with increasing temperature, which may be due to a decrease in fluid viscosity and a decrease in drag force with increasing temperature [29].

As shown in Figure 8, after adding AOS, the degree of migration in the migration stage is significantly reduced, and the overall permeability changes little; the permeability changes by about 0.5%, so the protective effect of surfactant AOS on the reservoir is obvious. Although the degree of migration increases with the increase in temperature, it is improved compared with that when AOS is not added, and it can be seen from the quartz electron microscope pictures treated with CO_2+AOS at 200°C that the degree of corrosion is much smaller. From the figure and the number of fines produced, it can also be shown that the chemical agent has a certain effect on the stability of the rock particles. From the infrared spectrum in Figure 5, it can be seen that the anionic surfactant AOS is adsorbed on the rock surface of the reservoir, and it shows the stability of porosity and permeability in rock physical properties as shown in Figure 8, while the porosity and permeability of the rock not adsorbed by AOS change greatly as shown in Figure 7, indicating that the role of chemical reagents in the tertiary oil recovery mechanism of CO_2 multicomponent thermal fluid is to act on the fluid on the one hand and stabilize the rock skeleton on the other hand. Its mechanism is shown in Figure 9. The ion exchange between rock mineral ions and cations in formation water makes the mineral surface absorb a large number of cations, which provides conditions for anionic surfactants to form a "protective layer."

4. Conclusions

Different minerals have different temperature responses to CO_2. It is difficult for CO_2 to dissolve quartz in a short time at high temperatures, and the dissolution rate is only about 0.1%, but the dissolution of clay is very strong. The degree of dissolution from large to small is illite, montmorillonite, and kaolinite, and the dissolution rate is above 1%. When AOS is added, this interaction is slowed down, and the dissolution rate becomes smaller.

During CO_2+steam injection, the porosity of the sand pack is inversely proportional to the temperature. AOS reduces the temperature response of the difference in porosity by half compared with that of CO_2+steam so that the reservoir porosity can be guaranteed not to change much during the superheated steam injection process. The change in permeability shows a trend of first decreasing and then increasing, which reflects the two migration stages of framework fines in the reservoir. Dissolution and migration as a leading factor or the migration of outflowing sand production become chief factors. The adsorption of AOS on the rock surface significantly slows down the damage of CO_2 to the rock under high-temperature steam, thereby improving the sudden change in permeability. Although there is still corrosion in steam+CO_2+AOS, this ensures that a part of CO_2 is stored in the reservoir, which also achieves the purpose of reducing CO_2 emissions.

The CO_2 multicomponent thermal fluid injection method is feasible in the subsequent development of thermal recovery of heavy oil reservoirs. On the basis of the fluid action mechanism, the CO_2 multicomponent thermal fluid injection method is supplemented to enhance the oil recovery mechanism. Especially, the steam+CO_2+AOS compound method can effectively alleviate the permeability heterogeneity in the unconsolidated sandstone and effectively reduce the degree of steam channelling.

Data Availability

The raw data used to support the conclusions of this study are available from the corresponding author upon request.

Conflicts of Interest

The authors declare that they have no conflicts of interest to report regarding the present study.

Acknowledgments

This work was financially supported by the National Natural Science Foundation of China (U20B6003).

References

[1] J. Hillier, C. Walter, D. Malin, T. Garcia-Suarez, L. Mila-i-Canals, and P. Smith, "A farm-focused calculator for emissions from crop and livestock production," *Environmental Modelling & Software*, vol. 26, no. 9, pp. 1070–1078, 2011.

[2] M. Adam, H. Anbari, A. Hart, J. Wood, J. P. Robinson, and S. P. Rigby, "In-situ microwave-assisted catalytic upgrading of heavy oil: experimental validation and effect of catalyst pore structure on activity," *Chemical Engineering Journal*, vol. 413, article 127420, 2021.

[3] M. L. Godec, V. L. Kuuskraa, and P. Dipietro, "Opportunities for using anthropogenic CO2for enhanced oil recovery and CO2 storage," *Energy & Fuels*, vol. 27, no. 8, pp. 4183–4189, 2013.

[4] Y. Z. Liu, Z. Rui, T. Yang, and B. Dindoruk, "Using propanol as an additive to CO_2 for improving CO_2 utilization and storage in oil reservoirs," *Applied Energy*, vol. 311, p. 118640, 2022.

[5] Y. Liu and Z. Rui, "A storage-driven CO2 EOR for a net-zero emission target," *Engineering*, vol. 18, pp. 79–87, 2022.

[6] X. Dong, H. Liu, Z. Chen, K. Wu, N. Lu, and Q. Zhang, "Enhanced oil recovery techniques for heavy oil and oilsands reservoirs after steam injection," *Applied Energy*, vol. 239, pp. 1190–1211, 2019.

[7] X. Dong, X. Jiang, W. Zheng et al., "Discussion on the sweep efficiency of hybrid steam–chemical process in heavy oil reservoirs: an experimental study," *Petroleum Science*, vol. 19, no. 6, pp. 2905–2921, 2022, in press.

[8] G. Bird, J. Boon, and T. Stone, "Silica transport during steam injection into oil sands: 1. Dissolution and precipitation kinetics of quartz: new results and review of existing data," *Chemical Geology*, vol. 54, no. 1-2, pp. 69–80, 1986.

[9] S. E. Taylor, "Interfacial chemistry in steam-based thermal recovery of oil sands bitumen with emphasis on steam-assisted gravity drainage and the role of chemical additives," *Colloids and Interfaces*, vol. 2, no. 2, p. 16, 2018.

[10] R. G. S. Araújo, J. L. A. O. Sousa, and M. Bloch, "Experimental investigation on the influence of temperature on the mechanical properties of reservoir rocks," *International Journal of Rock Mechanics and Mining Sciences*, vol. 34, no. 3-4, pp. 298.e1–298.e16, 1997.

[11] X. Dong, H. Liu, and Z. Chen, "Existing problems for steam-based enhanced oil recovery processes in heavy oil reservoirs," in *Hybrid Enhanced Oil Recovery Processes for Heavy Oil Reservoirs*, vol. 73 of Developments in Petroleum Science, , pp. 47–98, Elsevier, 2021.

[12] J. Fan, J. Yang, X. Fan, and L. Wu, "Experimental study on the mechanism of enhanced oil recovery by noncondensable gas-assisted steam flooding process in extra-heavy oil reservoir," *Energy Sources, Part A: Recovery, Utilization, and Environmental Effects*, vol. 43, no. 4, pp. 444–460, 2021.

[13] M. Guo, H. Liu, Y. Wang, H. Zhang, J. Wang, and X. Dong, "Sand production by hydraulic erosion during multicycle steam stimulation: an analytical study," *Journal of Petroleum Science and Engineering*, vol. 201, article 108424, 2021.

[14] X. I. Changfeng, Q. I. Zongyao, Y. Zhang et al., "CO_2 assisted steam flooding in late steam flooding in heavy oil reservoirs," *Petroleum Exploration and Development*, vol. 46, no. 6, pp. 1242–1250, 2019.

[15] Y. Liu, R. B. Grigg, and B. Bai, "*Salinity, pH, and surfactant concentration effects on CO2-foam*," Paper presented at the SPE International Symposium on Oilfield Chemistry, The Woodlands, Texas, 2005.

[16] H. D. Nejatian, E. Khodapanah, and E. Sahraei, "Experimental investigation of steam-CO2-foam flooding: combination of CO2-foam flooding and steam injection as an effective enhanced oil recovery (EOR) method in heavy oil reservoirs," *Asia-Pacific Journal of Chemical Engineering*, vol. 10, no. 3, article 377386, 2015.

[17] Z. Qi, T. Liu, C. Xi et al., "Status quo of a CO_2-assisted steam-flooding pilot test in China," *Geofluids*, vol. 2021, Article ID 9968497, 13 pages, 2021.

[18] C. Yanbin, L. Dongqing, Z. Zhang, W. A. Shantang, W. Quan, and X. Daohong, "Steam channeling control in the steam flooding of super heavy oil reservoirs, Shengli Oilfield," *Petroleum Exploration and Development*, vol. 39, no. 6, pp. 785–790, 2012.

[19] J. Zhao, F. Torabi, and J. Yang, "The role of emulsification and IFT reduction in recovering heavy oil during alkaline-surfactant-assisted CO_2 foam flooding: an experimental study," *Fuel*, vol. 313, article 122942, 2022.

[20] M. D. Reichert and L. M. Walker, "Interfacial tension dynamics, interfacial mechanics, and response to rapid dilution of bulk surfactant of a model oil–water-dispersant system," *Langmuir*, vol. 29, no. 6, pp. 1857–1867, 2013.

[21] D. B. Bennion, F. Thomas, and D. Sheppard, "Formation damage due to mineral alteration and wettability changes during hot water and steam injection in clay-bearing sandstone reservoirs," Paper presented at the SPE Formation Damage Control Symposium, Lafayette, Louisiana, 1992.

[22] J. Han, F. Feng, M. Yan, Z. Cong, S. Liu, and Y. Zhang, "CO_2-water-rock reaction transport via simulation study of nanoparticles-CO_2 flooding and storage," *Sustainable Energy Technologies and Assessments*, vol. 50, article 101736, 2022.

[23] Y. Sun, L. Zhao, T. Lin et al., "Enhance offshore heavy oil recovery by cyclic steam-gas-chemical costimulation," *Paper Presented at the SPE Heavy Oil Conference and Exhibition*, 2011, Kuwait City, Kuwait, 2011, 2011.

[24] D. Watkins, L. Kalfayan, D. Watanabe, and J. A. Holm, "Reducing gravel pack and formation dissolution during steam injection," *SPE Production Engineering*, vol. 1, no. 6, pp. 471–477, 1986.

[25] B. Fermaniuk, M. Claerhout, and D. Zhu, "In-situ SAGD thermal-chemical effects and metal-bond coated slotted liner design for enhanced sand control, flow and long-term performance," Paper presented at the SPE Thermal Well Integrity and Design Symposium, Banff, Alberta, Canada, 2015.

[26] M. A. Tabar, H. Bagherzadeh, A. Shahrabadi, and S. Dahim, "A comprehensive research in chemical consolidator/stabilizer agents on sand production control," *Journal of Petroleum Exploration and Production Technology*, vol. 11, no. 12, pp. 4305–4324, 2021.

[27] V. Lightbown, "New SAGD technologies show promise in reducing environmental impact of oil sand production," *Journal of Environmental Solutions for Oil, Gas, and Mining*, vol. 1, no. 1, pp. 47–58, 2015.

[28] D. Xiao-Hu and L. Hui-Qing, "Investigation of the features about steam breakthrough in heavy oil reservoirs during steam injection," *The Open Petroleum Engineering Journal*, vol. 5, no. 1, pp. 1–6, 2012.

[29] F. Bruns and T. Babadagli, "Heavy-oil recovery improvement by additives to steam injection: identifying underlying mechanisms and chemical selection through visual experiments," *Journal of Petroleum Science and Engineering*, vol. 188, article 106897, 2020.